Enhancing Welding Geometric Precision: Analyzing the Impact of Weld Path Directions, Sequences and Locating Schemes on Displacement

applied sciences

MDPI

Article

Enhancing Welding Geometric Precision: Analyzing the Impact of Weld Path Directions, Sequences and Locating Schemes on Displacement

Roham Sadeghi Tabar [1,*], Lars Lindkvist [1], Kristina Wärmefjord [1], Pasquale Franciosa [2], Dariusz Ceglarek [2] and Rikard Söderberg [1]

[1] Department of Industrial and Materials Science, Chalmers University of Technology, 41296 Gothenburg, Sweden
[2] Warwick Manufacturing Group (WMG), University of Warwick, Coventry CV4 7AL, UK
* Correspondence: rohams@chalmers.se

Abstract: Welding-induced geometric deviations remain a critical challenge in industrial manufacturing, particularly in achieving high-precision assembly. This study investigates the effects of welding path directions, sequences, and locating schemes on the displacement of welded assemblies, focusing on minimizing geometric deviations. Using finite element method (FEM) simulations and a design of experiments (DOE) approach, the interactions between these parameters were systematically analyzed. Results show that the locating scheme plays a dominant role in controlling displacement, with optimal configurations significantly reducing geometric errors. Welding sequences were also found to have a considerable impact, further minimizing distortions when appropriately optimized. The effect of weld path direction, while less significant for simpler geometries, became more pronounced in assemblies with curvature. These findings pinpoint the necessity of integrating a combined factor approach, including fixturing, welding sequence, and path direction, to optimize and improve the geometric quality of welded assemblies.

Keywords: weld path; locating schemes; sequence; geometric quality

Citation: Sadeghi Tabar, R.; Lindkvist, L.; Wärmefjord, K.; Franciosa, P.; Ceglarek, D.; Söderberg, R. Enhancing Welding Geometric Precision: Analyzing the Impact of Weld Path Directions, Sequences and Locating Schemes on Displacement. *Appl. Sci.* **2024**, *14*, 11144. https://doi.org/10.3390/app142311144

Academic Editor: Alberto Campagnolo

Received: 7 November 2024
Revised: 24 November 2024
Accepted: 27 November 2024
Published: 29 November 2024

1. Introduction

Welding is a fundamental industrial joining process involving the joining of materials, typically metals or thermoplastics, through the application of heat, pressure, or both. The geometric deviation of welding operations or other assembly operations directly influences the structural displacements of the final product due to the exerted heat and forces during the operation. Displacement during welding, which refers to the unintended movement or deformation of the workpiece, poses significant challenges, leading to dimensional inaccuracies and potential failures in welded structures [1–3].

Despite advancements in welding technologies, controlling and minimizing displacement remains a persistent issue. With the enhanced computational power, the state of the art focuses on combining data-driven models and physics-based simulation to control the geometric displacements during assembly [4–6]. Factors such as welding path directions [7], fixturing [8] of the workpiece, and welding sequences [9] interact, making the prediction and optimization of their combined effects complex on displacement. Traditional trial-and-error approaches to parameter optimization are time-consuming and resource-intensive, underscoring the need for more systematic and efficient methodologies.

1.1. Influence of Fixturing

The fixturing of the workpiece has a considerable impact in any assembly process [10]. The typical assembly process includes positioning the components in the fixture on a set of predefined coordinates, also known as the locating scheme, and clamping the parts.

Later, the parts are joined together, here by welding, and then released from the fixture. After releasing the parts from the fixture, springback will occur, and the final shape and displacement of the assembly will be determined [11,12]. Locating schemes play a crucial role in a product's robustness and are the main focus of the geometry assurance process [13]. The main purpose of the locating scheme is to lock degrees of freedom between the local part, sheet metal, and the target part, fixture, in a three-dimensional space. The scheme represents an orthogonal or non-orthogonal N-2-1 positioning system. In sheet metal assemblies, locating schemes are often over-constrained due to their non-rigid behavior to compensate for additional forces, i.e., gravity [14,15]. Several studies have been performed optimizing the fixturing points to reduce geometric deviation [16–19]. Phoomboplap and Ceglarek introduce a new approach to optimize fixture layout and thereby improve process yield in a given multistation assembly system. They emphasize the part and subassembly, locating stability and robustness to minimize product geometric variations. Franciosa et al. present a fixture capability measure to optimize the layout of locators and reference clamps, compensating for stochastic product variations and part deformation to improve assembly process yield and reduce the risk of product failures [17]. Xing introduces a fully automated method for optimizing fixture layouts by combining computer-aided tolerancing (CAT) simulation for dimensional analyses with global optimization algorithms, specifically the social radiation algorithm (SRA) and a genetic algorithm to enhance computational efficiency of the associated optimization problem [18]. Although several studies have studied the influence of fixturing, the interaction of the locating scheme and the welding parameters, namely, sequence and path direction, remains unexplored. In this study, the interaction between welding-related parameters and locating schemes is analyzed.

1.2. Influence of Welding Sequence

Welding sequence refers to the the order of applying the welds on a geometry. The sequence of the joining process is known to have a prominent impact on the distortion of the geometry [20]. The optimization of this sequence aims to determine the best joining sequence to achieve specific objectives, such as minimizing distortions or residual stresses. Due to the complexity of the problem, simulation-based methods are widely used, often combined with heuristic approaches derived from industrial practices. Early studies by Fukuda and Yoshikawa introduced a discrete method that divided the continuous welding path into smaller segments, optimizing the sequence to minimize local shrinkage and travel distance [20]. Subsequent research applied finite element simulations (FEM) to evaluate the effects of different sequences on distortion and stress in welded structures [21]. Various optimization algorithms, including genetic algorithms (GAs), have been employed to solve the combinatorial nature of the sequence problem for both continuous and point-based joining methods. Studies by Huang et al. [22] and Xie and Hsieh [23] applied a GA to reduce deformation and cycle time in spot welding, while others have focused on minimizing geometric deviation and variation in an assembly [24,25]. Similar to locating schemes, studies on welding sequences are often performed in isolation, disregarding the impact of the sequence parameters, which is addressed in this paper.

1.3. Influence of Weld Path

A weld path, or weld segment, is commonly encountered in continuous seam welding processes like TIG or laser welding. Each segment, also known as a weld pass, can be executed in either a forward or backward direction. To minimize distortion during welding, the weld paths that join components must be carefully selected [26,27]. This can involve breaking welds into shorter subwelds and adjusting the sequence and direction of these subwelds [9]. During welding, the localized heat causes expansion in the weld zone, while surrounding cooler areas restrain this expansion. As the weld cools, contraction occurs. The path of the weld determines how these expansions and contractions distribute within the structure, influencing the overall distortion patterns. The direction of the weld path

can either amplify or reduce the residual stresses created by thermal expansion and contraction [28]. If the weld path is planned to balance heat distribution, distortions can be minimized. The influence of the weld path and the sequence are often studied interconnected in an optimization framework, where FEM simulation models are often utilized to predict the behavior of the assembly [29,30]. Genetic algorithms have been studied extensively for the optimization of weld paths due to the similarity to the travelling salesman problem [29,31,32]. Asadi and Goldak proposed a surrogate model to solve the coupled weld sequence and weld path problem [7]. Wang et al. performed a literature review on the optimization of the weld path considering the cycle time for robot planning, where several studies are mentioned addressing the problem with a meta-heuristic algorithm [33]. This paper focuses on studying the influence of the direction of the weld path and sequence while considering the fixturing of the components to reduce distortion, which is the core structural optimization problem under investigation.

1.4. Scope of This Paper

This study focuses on evaluating the key assembly and welding parameters, specifically welding path directions, locating schemes, and welding sequences, to minimize displacement during welding processes. Although extensive research has been performed studying welding process parameters and their optimization individually, the coupled effect of the specified assembly parameters has not been studied. In this paper, using the design of experiments and finite element method (FEM) simulations, the interactions between the three parameters, weld sequence, path direction and locating schemes, is evaluated to understand their combined effects. The goal is to enhance the geometric quality and precision of welded structures by reducing displacement. The rest of this paper is organized to provide methods, results, discussion, conclusions, and future work.

2. Method

To study the impact of weld sequences, weld path direction, and locating schemes, a design of experiment (DOE) approach was taken. Due to the infeasibility of physical experiments for combinatorial problems, this study considered simulation experiments. The FEA simulation experiments were performed for the parameters, and the individual and coupled effects were studied. In the following, the details of the simulation model and the DOE approach are presented.

2.1. Welding Simulation

The simulation method utilized in this paper consists of two approaches. Initially, the fast response method was utilized for screening purposes. This approach integrates the new heat source model for keyhole mode laser welding presented in [34] with the Convex Volumetric Shrinkage (CVS) method for welding distortion simulation presented in [35]. The combined approach focuses on accurately simulating weld-induced distortions while ensuring computational efficiency. First, the heat input during welding is modeled using a combination of a Gaussian surface heat source and an upside-down cone to represent the "nail head" and the keyhole regions, respectively. The Gaussian heat source simulates the diffusive surface heat distribution, while the cone simulates the deeper penetration caused by the laser's keyhole effect. The heat input is governed by the following equations:

$$Q_s = \eta f_s Q,\ Q_c = \eta(1 - f_s)Q \tag{1}$$

where Q is the total power, f_s is the surface heat fraction, and η represents the efficiency. Next, the Convex Volumetric Shrinkage (CVS) method is employed to simulate the residual distortion induced by welding. The CVS method consists of three main steps: First, a steady-state thermal analysis is performed to calculate the temperature distribution along the weld path using a moving reference frame. The temperature above the melting point is used to identify the melt zone. Second, the melted zone is determined by identifying all nodes with temperatures above the melting point. A convex hull is generated around

these points to define the region of melted material. Thirdly, the melted zone is subjected to volumetric shrinkage as the material cools. This step assumes linear elastic shrinkage to predict the residual stresses and distortions. The temperature drop from the melting point to room temperature is applied uniformly to the nodes within the melted zone. This combination of a new heat source model with the CVS method provides an efficient, hence accurate, approach to simulate welding processes. This method is validated against experimental data, showing agreement in both weld bead geometry and residual distortions [34]. The CVS method significantly reduces computational time compared to full transient thermo-elasto-plastic simulations, making it suitable for applications requiring numerous simulations, such as variation analysis. To implement the above approach, a FEM simulation model was established, simulating the welding outcome with the above approach and screening the locating points.

The second approach involves full thermoplastic and transient simulation solving the heat transfer and the mechanical deformation at time steps for simulation of weld sequences and path directions. This method is also extensively validated by performing simulation and physical experiments [36]. The welding path is introduced to the model as a set of points of the geometry mesh, where the weld is applied and the direction of the weld path is set as the starting and end points in this set. Furthermore, the weld sequence is introduced by creating different sets of points representing the weld segments and applying the welding heat path to the segments in an orderly fashion. To represent the fixturing during the welding, the boundary conditions are applied to the nodes, locking the rotations and the translations in a given direction. The positioning system is introduced as six boundary conditions for each part included in the assembly. After welding is performed, the springback is calculated by negating the calculated after-weld displacement in the position of boundary conditions while the assembly is held in a measurement fixture. Figure 1 visualizes a model setup for welding experimentation, visualizing the weld paths, their sequences, and the locating schemes represented by the fixturing points.

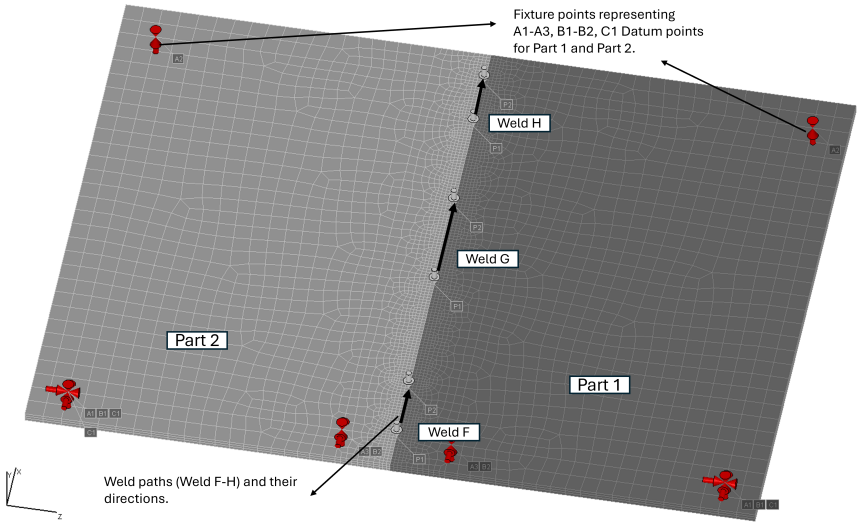

Figure 1. Assembly I—assembly of two INCONEL 718 metal plates with three weld segments F, G, and H.

2.2. Reference Assemblies

Assembly I consists of two metal parts. Three weld segments connect the parts together on the cross section of the two parts as butt welds. Figure 1 visualizes the prepared FEM model of the assembly. The basic geometry of the plates allows for understanding the locating scheme and welding sequence behavior. The positioning points for a near-optimal locating scheme are shown in Figure 1, with the thick arrows marked with A-B-C flags representing A, B, and C datum points. The welding paths and forward direction are

shown with the black arrows specified by Welds F–H, and the initial starting points and end points are shown by P1 and P2 for each segment. The sheet thickness for both parts is 3 mm. An ellipsoidal heat source, with a front length of 2, rear length of 4, width of 4, and depth of 1 mm, is utilized in this model. The weld geometry is considered as having a length of 1, width of 1, and height of 3 mm. The liquid and solid temperatures are set to 1523 and 1512 °C, respectively, and for the transient hull, the max temperature is set to 2000 °C with a keyhole feature of size 0.1 with a width of 4 and depth of 1 mm.

Assembly II consists of two metal parts. Three butt-weld segments connect the parts together at the position of the interface of the two parts. Figure 2 visualizes the prepared FEM model of the assembly. This assembly has more curvature and complex geometries and has an industrial use case in the aerospace industry. The positioning points for the near-optimal locating scheme, the welding paths in the forward direction of Welds F–H, and the initial starting points and end points are shown. The thickness for both parts is 3 mm. An ellipsoidal heat source, with a front length of 2, rear length of 4, width of 4, and depth of 1 mm, is utilized in this model. The weld geometry is considered as having a length of 0.2, width of 6, and height of 0.4 mm. The liquid and solid temperatures are set to 1300 °C, and for the transient hull, the max temperature is set to 2000 °C with a keyhole feature of size 0.1 with a width of 4 and depth of 1 mm. The material of the parts for both assemblies is nickel–chrome-based super alloy INCONEL 718.

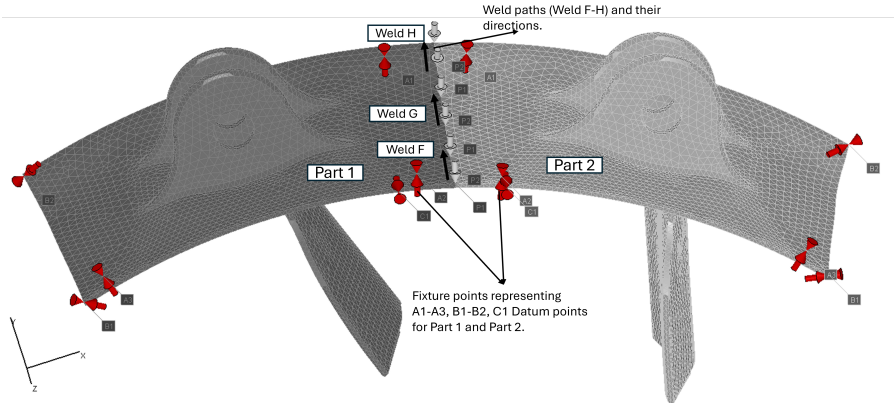

Figure 2. Assembly II—assembly of two INCONEL 718 metal parts with three weld segments F, G, and H.

In order to identify three levels of the locating scheme, an isolated screening of the parameter is performed. For this, the 6 locating points and their directions are considered as a decision variable in a Bayesian optimization routine to minimize the root mean square (RMS) of displacements in all the FEM nodes in the assembly. This displacement corresponds to the displacement of the assembly after welding and releasing the parts from the given locating scheme. Therefore the reported displacements are after cooling and springback. This screening was performed with a CVS approach where the simulation is not time-dependent, and thereby, the influence of the sequences and weld path direction is not taken into consideration. For Assembly I, 100 runs were performed to screen the behavior of the assembly using the different locating scheme inputs. For Assembly II, this screening was performed for 500 runs due to the geometric complexity of the assembly. The outcome of this screening is presented in Figure 3. For Assemblies I and II, three and two locating schemes from the lower and upper bounds and the mean of the screening outcome were chosen, respectively, representing near-optimal (N-O), mean, and non-ideal (N-I) solutions for the DOE presented in the next section. These levels for both assemblies are shown in Figure 3a,b.

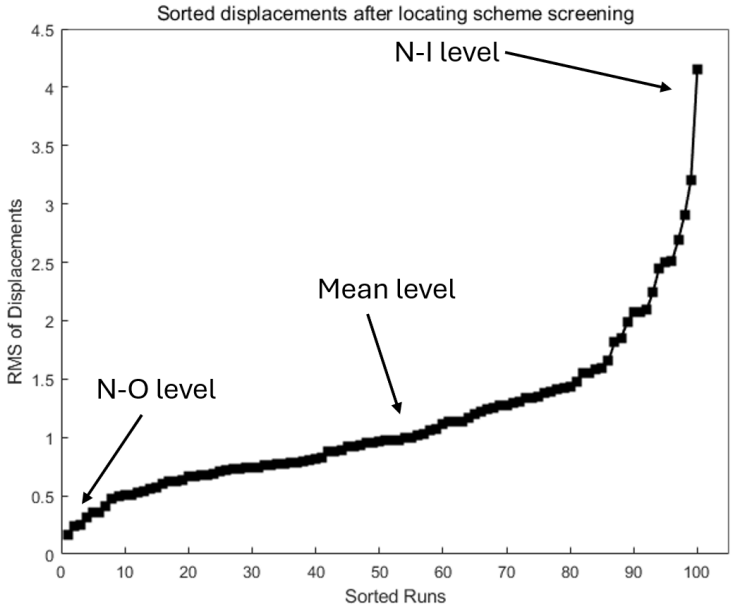

(a)

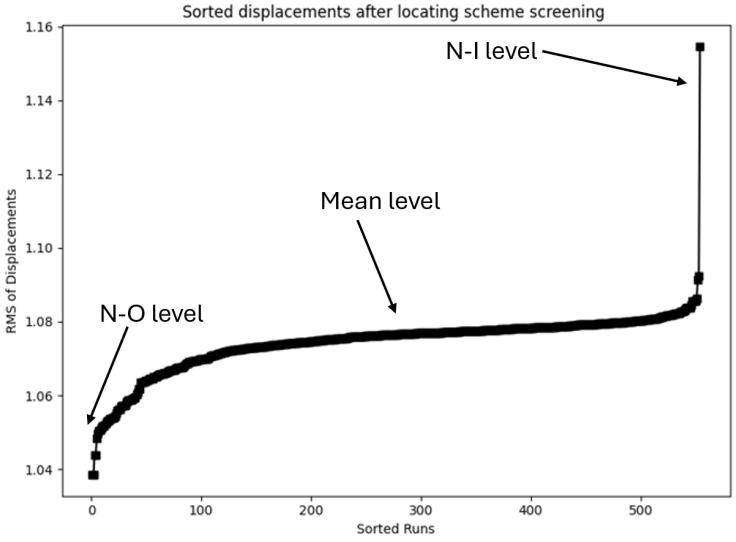

(b)

Figure 3. Screening of the locating scheme parameter with respect to the RMS of the displacements after welding and springback for the reference assemblies. (**a**) Reference Assembly I, (**b**) Reference Assembly II.

2.3. Design of Experiments

This study employed the Taguchi orthogonal array approach to study the aforementioned welding parameters affecting displacement. The approach, renowned for its efficiency in designing robust experiments, was selected to systematically evaluate the influence of multiple factors with a minimal number of experiments [37]. An L36 orthogonal array was utilized, accommodating five factors, where three represented the welding direction at two levels, forward and reverse. The locating scheme factor was represented by three levels, where we introduced three locating scheme layouts: non-ideal (N-I); mean, representing a solution close to the mean displacements during screening; and near-optimal (N-O). These layouts were derived from an optimization routine identifying the optimal locating scheme layouts. Finally, the welding sequence included three levels of combinations of the weld path segments, F, G, and H, to assess their individual and interactive

effects on welding displacement. The three sequences were derived after evaluating all the sequence combinations and choosing the solutions that resulted in optimal (N-O), non-ideal (N-I), and median displacement. Five key factors were identified as critical to welding displacement and studied in this paper, and they are listed in Table 1.

Table 1. Sequence optimization results.

Factor	Description	Levels
G	Path G direction	−1: reverse, 1: forward
H	Path H direction	−1: reverse, 1: forward
F	Path F direction	−1: reverse, 1: forward
E	Locating scheme	3 levels: 0: mean, 1: N-I, 2: N-O
S	Welding sequence	3 levels: 0: median, 1: N-I, 2: N-O

For Assembly II, due to the complexity of the geometry and enhanced simulation times, the locating scheme and welding sequences were reduced to two levels, N-I and N-O. The analysis in the second assembly is focused on the evaluation of the main effects. The welding simulation experiments were conducted using INCONEL 718 alloy, chosen for its high-temperature strength and corrosion resistance. The welding experiment used an ellipsoidal heat source with a power of 2.5 KW and an effect of 75%. The details of the heat source model are specified for each assembly in Section 2.2. A total of 36 simulation experimental runs were performed following the L36 orthogonal array design for Assembly I and L8 for Assembly II. Each run corresponded to a unique combination of factor levels as specified in the experimental design. The welding simulation was carried out under controlled conditions, changing the parameters according to the experimental plan. The complete plan is provided in Appendix A. Post-welding after springback, displacement as the root mean square of displacement in all the nodes was measured using the full transient FEM simulation.

2.4. Data Analysis

The collected data underwent several preprocessing steps to ensure their suitability for statistical analysis. The binary weld path factors F, G, H, were encoded as −1 and 1 to represent the two levels, the reverse and forward directions. The locating scheme, factor D, was encoded using one-hot encoding, creating separate dummy variables for each level, reference, N-I, and N-O, while excluding the reference category to avoid multicollinearity. The welding sequence factor E was encoded into three dummy variables corresponding to each welding sequence combination for Assembly I and two variables for Assembly II. After gathering all the required experiment data, the statistical analysis was conducted to assess multicollinearity among predictors. As capturing high-order interactions between the factors results in model instability due to the limited data in this experimental design, model reduction was utilized to capture the effect of the most significant factors and their interactions. For this purpose, the variance inflation factor (VIF) was calculated for each predictor to determine multicollinearity levels among the factors. Later, the analysis of variance (ANOVA) approach was taken to identify the significant main effects and interactions influencing welding displacement. The ANOVA model included main effects and significant interactions based on initial screening. To verify the assumptions of ANOVA, including normality and homoscedasticity, the residual plots were captured and evaluated. Furthermore, the normal quantile–quantile plot was established to evaluate the normality of residuals. Later, the plots of the main effects and interaction plots were utilized to further evaluate the influential factors. All data analysis was conducted using Python, utilizing the statmodels package for statistical modeling and ANOVA.

3. Results

The orthogonal array for the L-36 and L-8 experiments was established according to Section 2.3, and the simulation model was established following the methods in Section 2.1

for the two reference assemblies, Section 2.2. For Assemblies I and II, the summary statistics of the gathered data are presented in Table 2. The descriptive statistics for the root mean square (RMS) of the displacement in all the nodes by changing the parameters of weld path direction, weld sequences, and locating schemes, according to the DOE plan, are summarized in Table 2. The range of the displacement is 0.4714 mm, compromising 80% for the maximum displacement achieved. For the second assembly, the range of the displacement achieved is 4.293 mm, which compromises 84% of the maximum displacement achieved. This overview provides insight into how much a potential optimization of the parameters can improve the geometric accuracy after welding.

Table 2. Summary statistics of DOE data.

Statistic	Disp. Assembly I	Disp. Assembly II
Mean	0.275 mm	2.218 mm
Standard deviation	0.183 mm	1.761 mm
Minimum	0.117 mm	0.804 mm
Maximum	0.588 mm	5.097 mm
Median	0.172 mm	1.540 mm

Preliminary screening with the regression model revealed that the higher-order interactions could not be taken into consideration due to perfect multicollinearity between the parameters as the outcome of the VIF analysis. For this reason, the models were reduced to take into account only the interactions among the significant parameters. For Assembly I, the ANOVA model considered the main factors, including the welding sequences, the locating schemes, and the weld path direction of weld segments F and G. Weld segment H's direction was insignificant and was left out from the model. The two-way interaction between the welding sequences and the locating scheme were also included in the linear regression model as predictors. To evaluate multicollinearity among the predictors, the VIF was calculated for each predictor. All VIF values were below the threshold of 5, indicating low to moderate multicollinearity within the model. The VIF results are presented in Table 3. For Assembly II, due to the geometric complexity and simulation time, the number of experiments was reduced, and therefore only the main effects were studied.

Table 3. Variance inflation factor (VIF) for each predictor.

Predictors	VIF Assembly I	VIF Assembly II
F weld path	1	1
G weld path	1	1
Locator scheme N-O	1.33	1
Locator scheme mean	1.33	1
Sequence N-O	1.33	1
Sequence N-I	1.33	1
Locating scheme N-O and weld sequence N-O	1.78	N/A
Locating scheme mean and weld sequence N-O	1.78	N/A
Locating scheme N-O and weld sequence N-I	1.78	N/A
Locating scheme mean and weld sequence N-I	1.78	N/A

3.1. ANOVA Analysis

To determine the significance of the main effects and interaction effects on welding displacement, an ANOVA was conducted. The null hypothesis assumes that the factors under study do not affect the response variable. The results of the ANOVA are detailed in Table 4.

Table 4 clearly provides insight into the dominating factors contributing to the variation in the results, where the locating scheme has a significant dominance among other predictors given the large F-statistics and small p-Values ≤ 0.05. With the same analysis,

the direction of the weld path appears to be negligible given the small F-values and the relatively larger *p*-Values.

Table 4. ANOVA results for welding displacement.

Predictor	Sum of Squares	df	B	*p*-Value
Assembly I				
Locating scheme	13.08	2	3088.95	0
Sequence	0.30	2	70.37	0
Main weld path (F)	0.01	1	1.60	2.17×10^{-1}
Secondary weld path (G)	0.01	1	0.21	5.52×10^{-1}
Locating scheme and sequence	0.25	4	29.65	3.66×10^{-9}
Assembly II				
Locating scheme	15.46	1	182.74	0.0054
Sequence	3.02	1	35.75	0.0268
Main weld path (F)	3.03	1	35.89	0.0267
Secondary weld path (G)	0.003	1	0.04	0.8637
Tertiary weld path (H)	0.008	1	0.01	0.7804

3.2. Residual Analysis

Figure 4 displays the residuals plot for Assembly I, where a larger dataset is available. The residuals plotted against the fitted values exhibit a random scatter around the zero line without any discernible patterns or systematic structures. This randomness indicates that the assumptions of constant variance of residuals and linearity are satisfied. The consistent spread of residuals across all levels of fitted values suggests that the model adequately captures the underlying relationship between the predictors and the response variable.

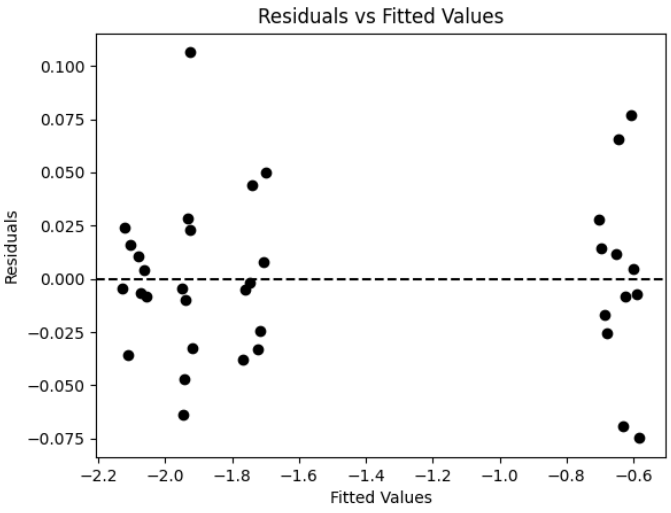

Figure 4. Residual-fitted plot for reference Assembly I.

Figure 5 presents the normal Q-Q plot for the residuals. This plot reveals that most of the residuals align closely along the reference line, indicating that they are approximately normally distributed. This alignment suggests that the normality assumption of the residuals is reasonably satisfied, which is crucial for the validity of parametric tests within the regression framework. Minor deviations observed at the tails of the distribution indicate slight departures from normality, which are common in practical data analysis. These minor deviations are unlikely to significantly impact the results due to the robustness of statistical tests against mild violations of normality. Overall, the approximate normality of the residuals confirms the appropriateness of the linear regression model and supports the validity of the hypothesis tests and confidence intervals computed in the analysis.

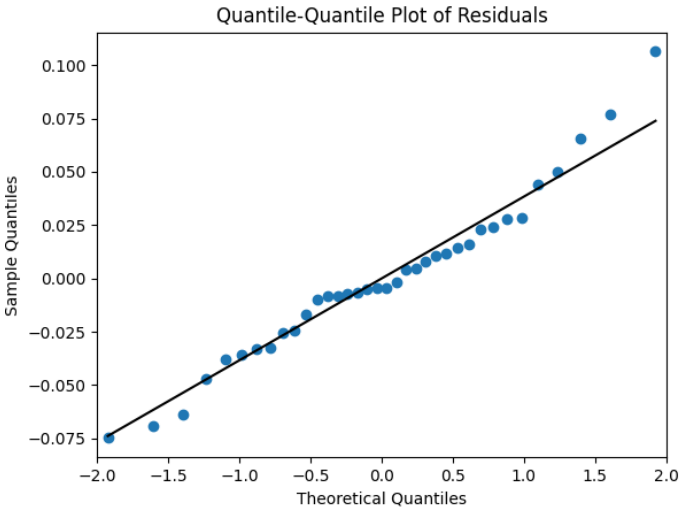

Figure 5. Quantile–quantile plot for reference Assembly I.

Furthermore, the plots of the main effects and the significant interactions were generated to visualize the influence of each factor on welding displacement. Figure 6 illustrates the main effects of the locating scheme, Figure 6a, welding sequences, Figure 6b, weld path directions of the two dominant paths, Figure 6c,d, and the interaction of the most significant factors. For Assembly I, the significant factors were the locating scheme and the welding sequences, Figure 6e,f, respectively.

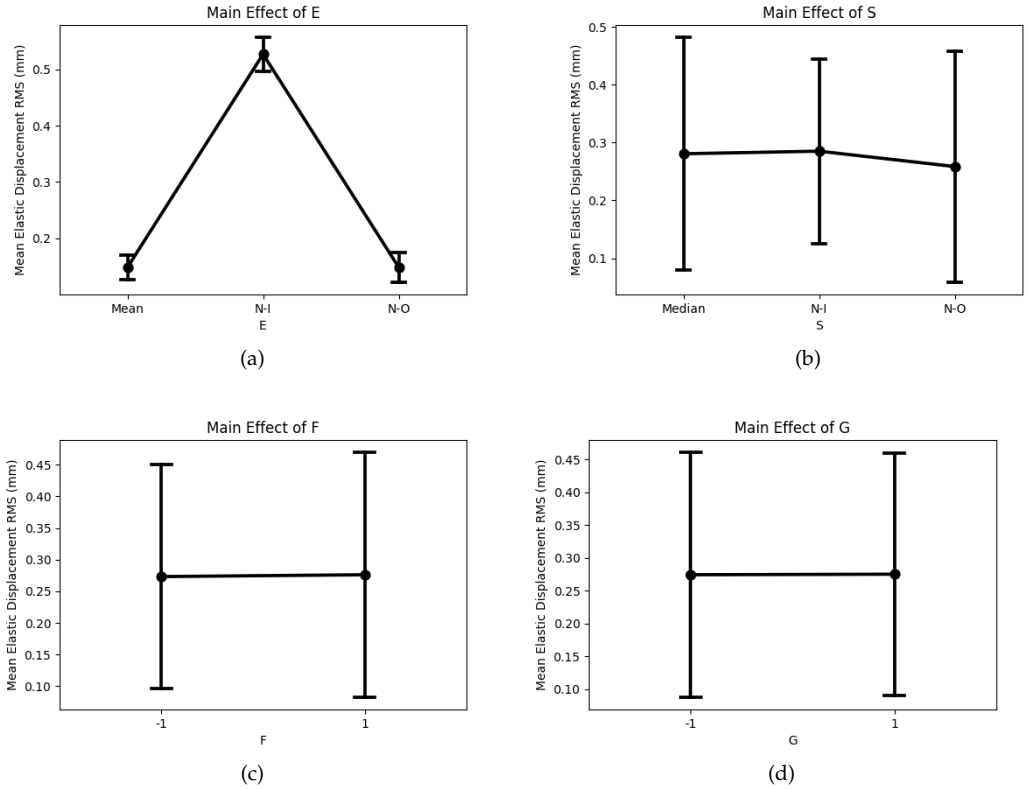

Figure 6. *Cont.*

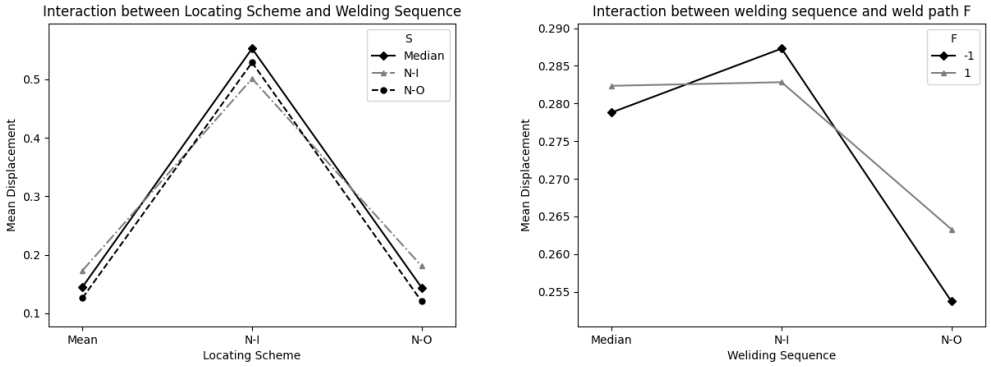

(e) (f)

Figure 6. Significant factors plot for Assembly I. (**a**) Locating scheme, (**b**) Welding sequence, (**c**) Weld path F direction, (**d**) Weld path G direction, (**e**) Interaction between locating scheme and sequence, (**f**) Interaction between sequence and weld F direction.

For Assembly II, the main effects were the locating scheme, visualized in Figure 7a, followed up by the weld sequence, in Figure 7b, and the weld paths F and G, in Figure 7c,d, respectively. The main interactions were between the locating scheme and the welding sequence visualized in Figure 7e and the interaction between the sequences and the weld path F's direction, Figure 7f.

In both assemblies, the locating scheme, representing the fixturing points and the orientation of those points, had a dominant influence on the displacements after welding and springback. The second main factor for both assemblies was the welding sequence, where changing the order of applying the weld segments was shown to have a significant effect on the displacement after springback. Finally, the weld path direction, where the forward or backward pass of the weld is determined, in both assemblies was shown to be relatively less significant for the displacements after welding and springback.

Figure 8a visualizes the displacements of the assembly welded in the N-O locating scheme and the optimal welding sequence and weld path direction. For Assembly I, this was welding the segments in the order of F (−), G (−), and H (−), where (−) indicates the backward direction. This is the opposite weld path direction shown in Figure 1. With these settings, the root mean square (RMS) of displacements in all the nodes was 0.1169 mm. Similarly, for the second assembly, the displacements with the N-O locating scheme and the optimal welding sequence and direction F (+), H (+), G (+) is shown in Figure 8b. The (+) sign indicates the forward weld path direction, as shown in Figure 2. The RMS of displacement for Assembly II with the specified settings was 0.804 mm.

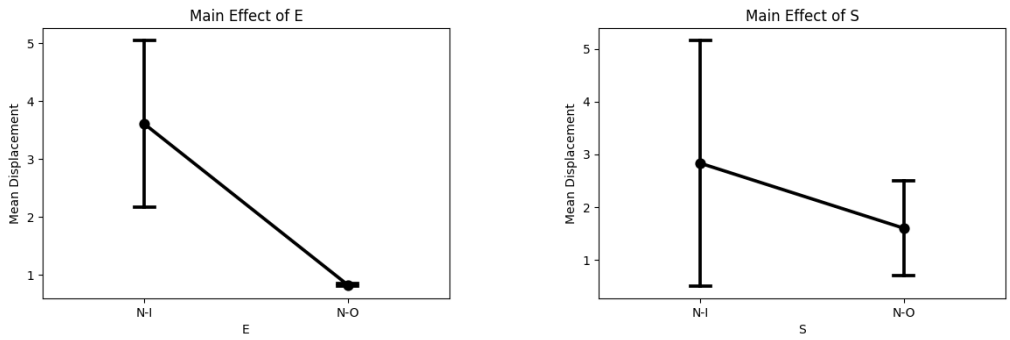

(a) (b)

Figure 7. *Cont.*

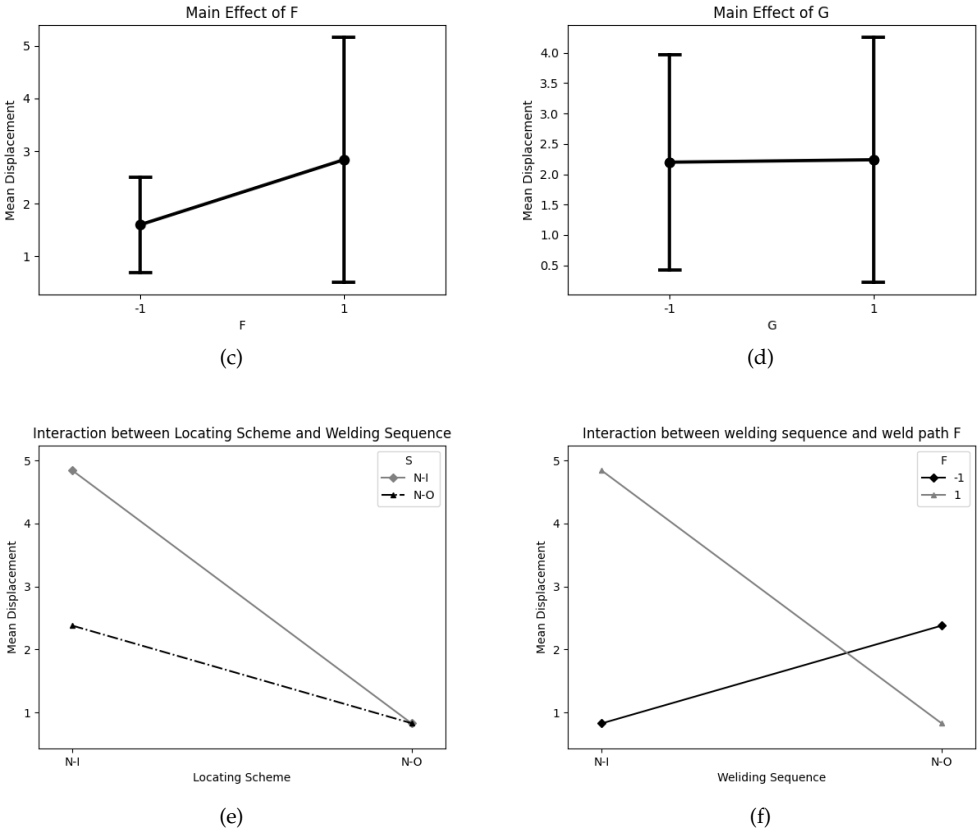

Figure 7. Significant factors plot for Assembly II, (**a**) Locating scheme, (**b**) Welding sequence, (**c**) Weld path F direction, (**d**) Weld path G direction, (**e**) Interaction between locating scheme and sequence, (**f**) Interaction between sequence and weld F direction.

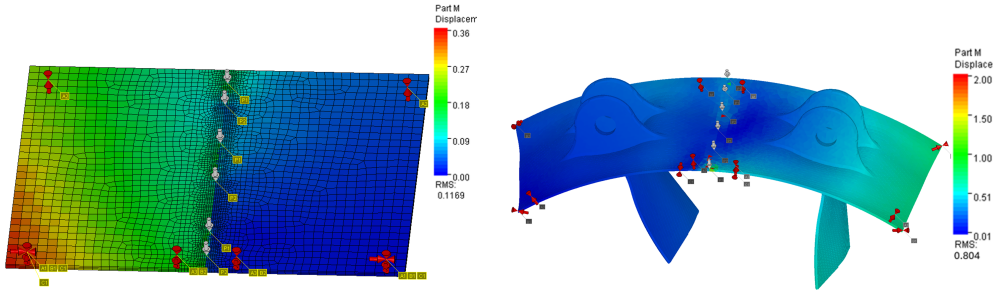

Figure 8. RMS of the displacements for the reference assemblies with the N-O parameter configurations, (**a**) Reference Assembly I, (**b**) Reference Assembly II.

4. Discussion

The primary objective of this study was to evaluate the design parameters affecting welding displacement using orthogonal arrays and simulation experiments. The analysis encompassed evaluating the effects of welding path directions, locating schemes, and welding sequences, along with their interactions. The results yielded several significant insights into the factors influencing welding displacement.

4.1. Interpretation of Main Effects

The locating scheme, factor E, exhibited an extremely significant effect on displacement after welding with close to zero *p*-Values, Table 4. Among the three levels, the near-optimal (N-O) solution derived from the initial screening's lowest displacements, followed by a

solution close to the mean value derived from the screening, resulted in lower displacement considering the welding sequence and direction of the welds. The real significance of the locating scheme on the outcome of the welding is prominent in a sensitive positioning system, which results in higher displacements, as visualized in Figures 6a and 7a. From the screening of the locating systems, it can also be seen that near-optimal solutions have a value closer to the mean of the displacements achieved with different locating scheme solutions, while a sensitive, as opposed to a robust, solution results in higher displacements, Figure 3. This analysis, in line with prior research on fixturing, indicates that a robust locating scheme can effectively minimize displacement by ensuring better alignment and stability during the welding process. The influence of locating schemes is consistent with prior studies highlighting the importance of fixture design and workpiece stability in reducing welding-induced distortions.

The welding sequence parameter also significantly influences displacement with close to zero *p*-Values, Table 4. The identification of the optimal welding sequence with a fixed locating scheme results in lower displacements. However, changing the locating scheme also changes the welding conditions, which means that an optimal welding sequence with one locating scheme does not necessarily result in lower displacements for all locating schemes. This behavior can be clearly seen in Figures 6b and 7b for both assemblies. This suggests that the order in which welding paths are executed needs to be optimized for a fixed locating scheme, which often occurs in practice. The welding sequence significantly influences heat distribution and residual stress minimization, thereby reducing overall displacement.

For the weld path direction, changing the forward and backward weld passes did not result in high variability in the experiments performed for Assembly I. The maximum range of displacement achieved by changing the path directions and keeping the locating scheme and the welding sequences constant was 0.094 mm. However, in Assembly II, where the weld was performed along a curvature, the path direction is shown to have significance. In Assembly II, the initial weld path F is shown to result in lower displacement when welded in the backward direction, opposite to what is shown in Figure 2. Furthermore, with the N-I locating scheme and the N-I welding sequence, changing the path direction resulted in a range of 0.516 mm. This result specifies that with sensitive locating schemes and N-I welding sequences, the significance of the weld path direction increases. Therefore, the optimization of displacements with respect to weld path direction, given the specified condition, will result in higher-quality improvements.

4.2. Interpretation of Interaction Effects

Due to the significance of the locating schemes on the overall displacements after welding, the interaction of the locating scheme with the other factors is of significance. The two main factors in Assembly I were the locating scheme and welding sequences. Figure 6e visualizes how these two interact for the N-O, N-I, and mean and median solutions for the locating scheme and the welding sequences. As can be seen, a near-optimal solution for the welding sequence resulted in lower displacements for the mean and N-O locating scheme solutions. However, in a non-ideal locating scheme, a non-ideal welding sequence resulted in minimum displacement, specifying the close interconnection between the locating scheme and the welding sequences. For Assembly II, the N-O locating scheme and N-O and N-I welding sequences resulted in similar displacement behavior; however, in the case of the N-I locating scheme, the N-O welding sequence helped to dampen the displacement by 56%, Figure 7e.

The interaction between Path F's direction, which had the highest significance among the three segments for both of the assemblies, and the welding sequences are studied in Figures 6f and 7f. This study shows that a backward pass resulted in lower displacement when the N-O (FGH) and median (HGF) welding sequences were utilized in Assembly I. For the N-I welding sequence in Assembly I (HFG), the forward weld path resulted in lower displacements. For Assembly II, the weld path F forward pass resulted in lower

displacement for the N-O welding sequence (FHG), and for the N-I welding sequence (GHF), the backward weld sequence resulted in lower displacement. This indicates that the effect of path direction on displacement varies depending on the welding sequence employed. This interplay underscores the necessity of considering combined factor effects rather than isolated influences when optimizing welding parameters.

4.3. Contribution Analysis

Based on the sum of squares (*ssq*) analysis achieved from the ANOVA results, presented in Table 4, a contribution analysis of the significant factors is established in Table 5. The sum of squares represents the total variability of each factor in the gathered experimental data. The contribution is calculated as

$$Contribution = \frac{ssq_i}{\sum ssq_i + \epsilon} \times 100, \quad (2)$$

where i represents each factor and ϵ is the residual *ssq* from the ANOVA analysis.

Table 5. Contribution analysis.

Predictor	Contribution
Assembly I	
Locating scheme	98.45 %
Sequence	2.19 %
Locating scheme and sequence	1.82 %
Main weld path (F)	0.07 %
Secondary weld path (G)	0.07 %
Residuals	0.39 %
Assembly II	
Locating scheme	71.80 %
Main weld path (F)	14.11 %
Sequence	14.04 %
Tertiary weld path (H)	0.03 %
Secondary weld path (G)	0.01 %
Residuals	8.51 %

Based on the contribution analysis presented in Table 5 and the ANOVA analysis and the supporting Figures 6 and 7, the following statements are derived:

- Locating schemes: Adopting optimal locating schemes can substantially reduce displacement, highlighting the importance of fixture design and workpiece stability in welding operations.
- Welding sequences: Strategic sequencing of welding paths can enhance displacement control.
- Directional control: Precise control over welding path directions is essential in minimizing displacement.
- Combined factors: The significant interactions underscore the necessity of a holistic approach in parameter optimization. The adjustment of one factor should consider the levels of interacting factors to enhance displacement minimization.

Despite the robust findings, it needs to be considered that the inclusion of all the interactions for combinatorial problems enhances the need for full factorial DOE plans. This complexity can both be computationally infeasible in simulation experiments and obscure the interpretability of individual predictor effects in the ANOVA context. Furthermore, while FEM simulations provide valuable insights, physical welding conditions may introduce additional variables and uncertainties not captured in the simulations. The inherent simulation inaccuracies also need to be included in the analysis of the results.

5. Conclusions

This study provided an in-depth analysis of how welding path directions, sequences, and locating schemes influence the geometric precision of welded assemblies. Utilizing finite element simulations and a design of experiments (DOE) approach, the individual and combined effects of these parameters on post-welding displacement were systematically evaluated. Among the factors studied, locating schemes emerged as the most critical determinant of geometric displacement, significantly influencing the final displacements and overall stability of welded components. Optimized locating schemes resulted in a substantial reduction in geometric deformation after welding and springback, ensuring that parts remained better aligned during and after the welding process. Welding sequences also played a key role in reducing displacements, highlighting the importance of determining an optimal order in which welds are applied to further minimize deformations. The influence of weld path directions was found to be less impactful compared to locating schemes and sequences, particularly in assemblies with simpler geometries. However, for assemblies with more complex shapes, such as those with curvature, the weld path direction demonstrated a more pronounced effect on geometric distortions. This suggests that while weld path direction might be of secondary importance in simpler cases, it becomes crucial in more intricate assemblies. Overall, this study emphasizes the importance of a combined, systematic approach in optimizing welding parameters to enhance geometric accuracy and reduce distortions in welded structures, resulting in precise and efficient welding processes in industrial applications.

Future research includes extending the current work to more complex geometries and materials and incorporating real-world physical experiments to validate the simulation results further. This study highlights the need to explore the interaction between more welding parameters, such as heat input and clamping forces, to refine the control of distortions. Additionally, integrating advanced real-time optimization algorithms, such as deep reinforcement learning, could further enhance the prediction and minimization of welding-induced distortions across a broader range of industrial applications.

Author Contributions: Conceptualization, R.S.T.; methodology, R.S.T., P.F., D.C., K.W. and R.S.; software, R.S.T. and L.L.; validation, R.S.T. and L.L.; formal analysis, R.S.T.; investigation, R.S.T.; resources, R.S.T.; data curation, R.S.T.; writing—original draft preparation, R.S.T., K.W. and R.S.; writing—review and editing, R.S.T., P.F., D.C., K.W. and R.S.; visualization, R.S.T.; project administration, R.S.T., D.C., K.W. and R.S.; funding acquisition, K.W. and R.S. All authors have read and agreed to the published version of the manuscript.

Funding: This research was funded by the Swedish Energy Agency, grant no. P2022-00228-Energi.

Institutional Review Board Statement: Not applicable.

Informed Consent Statement: Not applicable

Data Availability Statement: The data presented in this study are available on request from the corresponding author. The data are not publicly available due to privacy.

Acknowledgments: This work was carried out at the Wingquist Laboratory within the Area of Advance Production at Chalmers, Sweden, and in collaboration with Warwick Manufacturing Group (WMG) at the University of Warwick. The project is supported by the Swedish Energy Agency. The support is gratefully acknowledged.

Conflicts of Interest: The authors declare that the research was conducted in the absence of any commercial or financial relationships that could be construed as a potential conflict of interest.

Appendix A

The detailed simulation experimental plan is provided in the following table. For deriving the locating scheme and the welding sequence parameter settings over 100 simulation runs for Assembly I and 500 runs for Assembly II were performed, see Sections 2.2 and 2.3.

Table A1. Experimental plan.

Run	Welding Sequence	Locating Scheme	Path Direction F(+1/−1)G(+1/−1)H(+1/−1)
Assembly I			
1	FGH	N-O	+1, +1, +1
2	FGH	N-O	+1, −1, −1
3	FGH	N-O	−1, +1, +1
4	FGH	N-O	−1, −1, −1
5	HGF	N-O	+1, +1, −1
6	HGF	N-O	+1, −1, +1
7	HGF	N-O	−1, +1, −1
8	HGF	N-O	−1, −1, +1
9	HFG	N-O	+1, +1, +1
10	HFG	N-O	+1, −1, −1
11	HFG	N-O	−1, +1, +1
12	HFG	N-O	−1, −1,−1
13	FGH	Mean	+1, +1, −1
14	FGH	Mean	+1, −1, +1
15	FGH	Mean	−1, +1, v1
16	FGH	Mean	−1, −1, +1
17	HGF	Mean	+1, +1, +1
18	HGF	Mean	+1, −1, −1
19	HGF	Mean	−1, +1, +1
20	HGF	Mean	−1, −1, −1
21	HFG	Mean	+1, +1, −1
22	HFG	Mean	+1, −1, +1
23	HFG	Mean	−1, +1, −1
24	HFG	Mean	−1, −1, +1
25	FGH	N-I	+1, +1, +1
26	FGH	N-I	+1, −1, −1
27	FGH	N-I	−1, +1, +1
28	FGH	N-I	−1, −1, −1
29	HGF	N-I	+1, +1, −1
30	HGF	N-I	+1, −1, +1
31	HGF	N-I	−1, +1, −1
32	HGF	N-I	−1, −1,+1
33	HFG	N-I	+1, +1, +1
34	HFG	N-I	+1, −1, −1
35	HFG	N-I	−1, +1, +1
36	HFG	N-I	−1, −1, −1
Assembly II			
1	FHG	N-O	+1, +1, +1
2	FHG	N-O	+1, −1, −1
3	GHF	N-O	−1, +1, +1
4	GHF	N-O	−1, −1, −1
5	FHG	N-I	−1, +1, −1
6	FHG	N-I	−1, −1, +1
7	GHF	N-I	+1, +1, −1
8	GHF	N-I	+1, −1, +1

References

1. Murakawa, H.; Deng, D.; Ma, N.; Wang, J. Applications of inherent strain and interface element to simulation of welding deformation in thin plate structures. *Comput. Mater. Sci.* **2012**, *51*, 43–52. [CrossRef]
2. Brown, S.; Song, H. Finite Element Simulation of Welding of Large Structures. *J. Eng. Ind.* **1992**, *114*, 441–451. [CrossRef]
3. Deng, D.; Murakawa, H.; Liang, W. Numerical simulation of welding distortion in large structures. *Comput. Methods Appl. Mech. Eng.* **2007**, *196*, 4613–4627. [CrossRef]
4. Liu, S.; Wu, Z.; Zhou, W.; Zhou, H.; Zhang, K.; Yin, D.; Lei, Y.; Qiu, Y. A review of welding simulation methods for large components. *Prog. Nat. Sci. Mater. Int.* **2023**, *33*, 551–568. [CrossRef]

5. Zeng, Z.; Wang, L.; Du, P.; Li, X. Determination of welding stress and distortion in discontinuous welding by means of numerical simulation and comparison with experimental measurements. *Comput. Mater. Sci.* **2010**, *49*, 535–543. [CrossRef]
6. Chen, Z.; Yu, Q.; Luo, Y.; Shenoi, R.A. Comparative study of welding deformation of a stiffened panel under various welding procedures. *Proc. Inst. Mech. Eng. Part J. Eng. Manuf.* **2019**, *233*, 182–191. [CrossRef]
7. Asadi, M.; Goldak, J.A. Combinatorial optimization of weld sequence by using a surrogate model to mitigate a weld distortion. *Int. J. Mech. Mater. Des.* **2011**, *7*, 123–139. [CrossRef]
8. Yu, K.; Wang, X. Modeling and optimization of welding fixtures for a high-speed train aluminum alloy sidewall based on the response surface method. *Int. J. Adv. Manuf. Technol.* **2022**, *119*, 315–327. [CrossRef]
9. Voutchkov, I.; Keane, A.; Bhaskar, A.; Olsen, T.M. Weld sequence optimization: The use of surrogate models for solving sequential combinatorial problems. *Comput. Methods Appl. Mech. Eng.* **2005**, *194*, 3535–3551. [CrossRef]
10. Camelio, J.A.; Hu, S.J.; Ceglarek, D. Impact of fixture design on sheet metal assembly variation. *J. Manuf. Syst.* **2004**, *23*, 182–193. [CrossRef]
11. Li, B.; Shiu, B.; Lau, K. Robust fixture configuration design for sheet metal assembly with laser welding. *J. Manuf. Sci. Eng.* **2003**, *125*, 120–127. [CrossRef]
12. Govik, A.; Nilsson, L.; Moshfegh, R. Finite element simulation of the manufacturing process chain of a sheet metal assembly. *J. Mater. Process. Technol.* **2012**, *212*, 1453–1462. [CrossRef]
13. Söderberg, R.; Wärmefjord, K.; Carlson, J.S.; Lindkvist, L. Toward a Digital Twin for real-time geometry assurance in individualized production. *CIRP Ann.* **2017**, *66*, 137–140. [CrossRef]
14. Liu, S.C.; Hu, S.J. Variation simulation for deformable sheet metal assemblies using finite element methods. *J. Manuf. Sci. Eng.* **1997**, *119*, 368–374. [CrossRef]
15. Sadeghi Tabar, R.; Zheng, H.; Litwa, F.; Paetzold-Byhain, K.; Lindkvist, L.; Wärmefjord, K.; Söderberg, R. Digital twin-based clamping sequence analysis and optimization for improved geometric quality. *Appl. Sci.* **2024**, *14*, 510. [CrossRef]
16. Phoomboplab, T.; Ceglarek, D. Process Yield Improvement Through Optimum Design of Fixture Layouts in 3D Multistation Assembly Systems. *J. Manuf. Sci. Eng.* **2008**, *130*, 061005. [CrossRef]
17. Franciosa, P.; Gerbino, S.; Ceglarek, D. Fixture capability optimisation for early-stage design of assembly system with compliant parts using nested polynomial chaos expansion. *Procedia CIRP* **2016**, *41*, 87–92. [CrossRef]
18. Xing, Y. Fixture layout design of sheet metal parts based on global optimization algorithms. *J. Manuf. Sci. Eng.* **2017**, *139*, 101004. [CrossRef]
19. Mohan, A.; Franciosa, P.; Dai, D.; Ceglarek, D. A novel approach to control thermal induced buckling during laser welding of battery housing through a unilateral N-2-1 fixturing principle. *J. Adv. Join. Process.* **2024**, *10*, 100256. [CrossRef]
20. Fukuda, S.; Yoshikawa, K. Determination of welding sequence: A neural net approach. *Eng. Anal. Bound. Elem.* **1990**, *7*, 78–82. [CrossRef]
21. Mochizuki, M.; Hayashi, M.; Hattori, T. Residual stress distribution depending on welding sequence in multi-pass welded joints with X-shaped groove. *J. Pressure Vessel Technol.* **2000**, *122*, 27–32. [CrossRef]
22. Huang, M.W.; Hsieh, C.C.; Arora, J.S. A genetic algorithm for sequencing type problems in engineering design. *Int. J. Numer. Methods Eng.* **1997**, *40*, 3105–3115. [CrossRef]
23. Xie, L.S.; Hsieh, C. Clamping and welding sequence optimisation for minimising cycle time and assembly deformation. *Int. J. Mater. Prod. Technol.* **2002**, *17*, 389–399. [CrossRef]
24. Sadeghi Tabar, R.; Wärmefjord, K.; Söderberg, R.; Lindkvist, L. Critical joint identification for efficient sequencing. *J. Intell. Manuf.* **2021**, *32*, 769–780. [CrossRef]
25. Wu, C.; Wang, C.; Kim, J.W. Welding sequence optimization to reduce welding distortion based on coupled artificial neural network and swarm intelligence algorithm. *Eng. Appl. Artif. Intell.* **2022**, *114*, 105142. [CrossRef]
26. Pandey, C.; Giri, A.; Mahapatra, M. On the prediction of effect of direction of welding on bead geometry and residual deformation of double-sided fillet welds. *Int. J. Steel Struct.* **2016**, *16*, 333–345. [CrossRef]
27. Yang, B.; Alkhafaji, A.; Ma, J.; Wang, H.P.; Carlson, B.E.; Tong, W. A fixture design for controlling impact of the airflow on laser welding of galvanized steels. *Opt. Laser Technol.* **2025**, *181*, 111736. [CrossRef]
28. Colegrove, P.; Ikeagu, C.; Thistlethwaite, A.; Williams, S.; Nagy, T.; Suder, W.; Steuwer, A.; Pirling, T. Welding process impact on residual stress and distortion. *Sci. Technol. Weld. Join.* **2009**, *14*, 717–725. [CrossRef]
29. Islam, M.; Buijk, A.; Rais-Rohani, M.; Motoyama, K. Simulation-based numerical optimization of arc welding process for reduced distortion in welded structures. *Finite Elem. Anal. Des.* **2014**, *84*, 54–64. [CrossRef]
30. Fu, G.; Lourenço, M.I.; Duan, M.; Estefen, S.F. Influence of the welding sequence on residual stress and distortion of fillet welded structures. *Mar. Struct.* **2016**, *46*, 30–55. [CrossRef]
31. Yang, H.; Shao, H. Distortion-oriented welding path optimization based on elastic net method and genetic algorithm. *J. Mater. Process. Technol.* **2009**, *209*, 4407–4412. [CrossRef]
32. Kadivar, M.; Jafarpur, K.; Baradaran, G. Optimizing welding sequence with genetic algorithm. *Comput. Mech.* **2000**, *26*, 514–519. [CrossRef]
33. Wang, X.; Zhou, X.; Xia, Z.; Gu, X. A survey of welding robot intelligent path optimization. *J. Manuf. Process.* **2021**, *63*, 14–23. [CrossRef]

34. Lorin, S.; Madrid, J.; Söderberg, R.; Wärmefjord, K. A new heat source model for keyhole mode laser welding. *J. Comput. Inf. Sci. Eng.* **2022**, *22*, 011004. [CrossRef]
35. Lorin, S.; Cromvik, C.; Edelvik, F.; Lindkvist, L.; Söderberg, R. Variation simulation of welded assemblies using a thermo-elastic finite element model. *J. Comput. Inf. Sci. Eng.* **2014**, *14*, 031003. [CrossRef]
36. Goldak, J.; Asadi, M. Challenges in validation of computational weld mechanics code to compute residual stress and distortion in welds. *J. Press. Vessel. Technol.* **2014**, *136*, 011201. [CrossRef]
37. Taguchi, G.; Chowdhury, S.; Wu, Y. Introduction to Orthogonal Arrays. In *Taguchi's Quality Engineering Handbook*; John Wiley and Sons, Ltd.: Hoboken, NJ, USA, 2004; Chapter 35, pp. 584–596. [CrossRef]